

## The effect of different levels of cleanliness of the pre-coat surface on adhesion and corrosion performance of A36 steel with epoxy coating



Teguh Dwi Widodo\*, Putu Hadi Setyarini, Sugiarto Sugiarto, Rudianto Raharjo, Redi Bintaro, Djarot Bangun Darmadi, Sagita Sagita

Department of Mechanical Engineering, Faculty of Engineering, Universitas Brawijaya, Indonesia

### Abstract

Adhesion and corrosion protection are the main properties of epoxy coatings, especially when applied to materials exposed to harsh environments, such as chloride-containing water. However, the adhesion and corrosion protection of coatings are affected by surface preparation, especially the cleanliness of the substrate surface prior to coating application. Choosing the proper surface preparation can optimize the coating's capabilities. This research aims to evaluate the Effect of blasting process cleanliness on coating performance on the steel surface. The novel approach is to correlate NACE surface cleanliness standards with coating performance. In this study, A36 steel is used. The cleaning procedure uses an air-blasting process with an 8-bar nozzle pressure and at least 5 minutes of spraying time to meet the desired National Association of Corrosion Engineers (NACE) standard. The abrasive utilizing garnet with a mesh of 30-40. Meanwhile, coating is performed at room temperature using the airless spray method with a 90° angle, a distance of 25 cm from the substrate and the nozzle, and a nozzle speed of 300 mm/s. The gap in the coating process between the first and second layers is 24 hours. The results showed that surface preparation influenced the coating's pullout strength and corrosion performance. The pullout strength test demonstrated that NACE 2 provided the highest pullout strength. Likewise, corrosion rate testing showed that surface preparation affects the corrosion rate, with NACE 1 providing the lowest corrosion rate (the best corrosion protection).

### Keywords:

A36 Steel;  
Adhesion Strength;  
Coating Layer Thickness;  
Corrosion Rate;  
Surface Cleanliness;

### Article History:

Received: April 21, 2025  
Revised: August 29, 2025  
Accepted: September 12, 2025  
Published: January 12, 2026

### Corresponding Author:

Teguh Dwi Widodo  
Department of Mechanical  
Engineering, Faculty of  
Engineering, Universitas  
Brawijaya, Indonesia  
Email:  
[widodoteguhdwi@ub.ac.id](mailto:widodoteguhdwi@ub.ac.id)

This is an open-access article under the [CC BY-SA](https://creativecommons.org/licenses/by-sa/4.0/) license.



### INTRODUCTION

The hull represents the most significant structural component of a ship. The hull is the ship's watertight covering that safeguards the cargo hold, machinery, and accommodations from the detrimental effects of weather, flooding, and structural damage [1]. The hull, regardless of the material employed, must be adequately resilient to withstand the complete spectrum of loads encountered over a ship's operational lifespan [2, 3, 4]. A36 steel is widely used in ship hulls today. ASTM A36 steel is a low-carbon steel

that exhibits favorable strength and deformation properties. However, A36 steel has a weakness, particularly in terms of corrosion resistance.

The hull surface is a ship's part that is more susceptible to corrosion than other parts. In addition to corrosion, marine microorganisms can readily grow on surfaces, leading to fouling [5]. It is imperative that these factors be managed and that maintenance be conducted regularly to prevent hull damage [6].

Corrosion in maritime environments poses significant risks to the integrity and longevity of

ships, primarily due to the interaction between seawater and the metallic materials used in ship construction. This interaction can lead to various forms of corrosion, including pitting, crevice corrosion, and microbiologically influenced corrosion [7][8]. The economic impact of corrosion is substantial, as corrosion-related issues can incur costs far exceeding the direct costs of prevention and mitigation strategies [9].

The corrosion process in ship materials, particularly in aluminum alloys and steel, is influenced by environmental factors and the presence of microorganisms and Chloride ions. For instance, the presence of saltwater increases electrochemical activity, thereby accelerating corrosion rates [10]. Additionally, microorganisms, such as certain bacteria, can exacerbate corrosion by altering local chemical environments and accelerating electrochemical reactions [11]. These microbial activities can initiate localized corrosion, including pitting and galvanic corrosion, through anodic and cathodic reactions facilitated by biofilms [12].

Various protective methods are employed, including the application of organic coating to combat corrosion processes [13][14]. Studies demonstrate that these coatings not only prevent corrosion at flaws but also form protective layers that remain effective even under extended exposure to corrosive environments [15][16]. Coating is defined as the process of applying a protective layer to a base material (substrate) to prevent corrosion and provide additional protection [17]. Coatings used in the maritime sector must demonstrate resistance to a wide range of environmental factors, including seawater, brackish water, harbor water, and dirt [18].

One principal function of organic coating is to form a barrier that limits the ingress of water and corrosive ions, such as chlorides and sulfates, which are known to promote corrosion [19][20]. Bonding between epoxy coatings and metal substrates is a persistent issue, as insufficient adhesion can lead to delamination. Surface roughening has demonstrated the ability to augment bonding strength between coatings and substrates, hence enhancing corrosion resistance. Likewise, applying primer coats can improve the interface by prepping the substrate surface, thereby enhancing adhesion. This procedure is categorized as surface preparation, defined as any technique utilized to ready a surface for coating [21]. Before applying the coating, it is essential to remove all residual oil, grease, dirt, rust, and other contaminants from the surface through surface preparation. Surface preparation can be achieved using a high-

pressure cleaning apparatus or water blasting [22]. Blast cleaning is the act of cleaning a surface with abrasive particles (jets). Blasting is an effective method for removing contaminants, debris, corrosion, and old coatings [23]. Meanwhile, abrasive particles commonly used include sand; other fine materials, including copper slag, shot, glass, metal, dry ice, garnet, and coconut shell or plant fragments, can also be employed [24].

Research specifically focuses on models that quantify the cleanliness attained through blasting, and its relationship with coating performance is limited [25]. Although standards such as ISO 8501-1 and the National Association of Corrosion Engineers (NACE) provide visual guidelines for surface cleanliness, they do not offer measurable models for cleanliness levels in terms of adhesion strength or corrosion resistance. Moreover, existing research focuses solely on the influence of surface roughness on paint-substrate adhesion, but little is known about the effects of cleanliness on coating bond strength and corrosion [26, 27, 28, 29]. No research was found that discusses the Effect of cleanliness on the specific A36 steel material.

The novelty of this research lies in examining the corrosion properties of A36 steel and the pullout strength of the epoxy applied to its surface as a function of surface cleanliness prior to coating. The cleaning procedure impacts the cleanliness itself during garnet blasting. Moreover, corrosion characterization employs a new quantitative approach, potentiodynamic polarization, which measures the corrosion rate and material nobility to assess anodic characteristics, rather than traditional methods such as weight loss and visual assessment.

## METHOD

### Material

The substrate employed in this investigation was A36 carbon steel, characterized by a chemical composition of 0.26% C, 0.29% Si, 1.05% Mn, 0.04% P, and 0.07% S, with iron as the balance (wt.%) supplied by Krakatau Steel. Before the cleaning process, the steel is soaked in seawater to produce rust, so that it resembles the material used on a ship's hull. Meanwhile, the epoxy coatings employed in this study were formulated with polyamides and zinc particles. The epoxy coat was supplied by International Coating, AkzoNobel, the Netherlands, and the zinc particles were supplied by Sigma-Aldrich, which are 99% zinc oxide. Meanwhile, the NaCl solution for the corrosion test was prepared by adding scientific-grade NaCl (High purity)

supplied by Merc, USA, to Demineralized Water with 3.5% wt.

## Methods

The research process is illustrated in Figure 1. Prior to the application of the coating, the A36 was dimensionally cut to 20 cm x 10 cm x 0.5 cm and subjected to abrasive blasting using garnet dry blasting, followed by comparing the blasting result with the NACE cleanliness standard to obtain the desired surface cleanliness according to various cleanliness standards (NACE 1, NACE 2, NACE 3, NACE 4). The processes are then followed by rinsing the substrate with 70 wt.% ethanol. The pressure for garnet blasting is 8 bar, with garnet of mesh size 30-40. The spraying angle is 90° with a distance of 30 cm. Spraying time is at least 5 minutes to achieve the desired NACE standard.

The research process was then followed by the preparation of the epoxy coating, which was created by combining epoxy coating and polyamide hardener in a mass ratio of 4:1 and mixed with 5% wt. of zinc powder. The coating application on the A36 substrate follows the next step. The epoxy was applied using a coating film applicator, whose basic mechanism is airless spray. The coating process is performed at room temperature using the airless spray method at a 90° angle, with a distance of 25 cm and a nozzle movement speed of 300 mm/s. Samples were kept at room temperature for 24 h after the first coating was applied, and then another layer of epoxy was applied on the first Layer. The samples were left at room temperature (25 °C) for 7 days before undergoing the Pullout test, Corrosion Test, and optical observation. Meanwhile, coating thickness was measured in wet and dry conditions using a PosiTector® 6000 from Defelsko.

The pullout test was performed on all specimens using a PosiTector AT-M from Defelsko, in accordance with ASTM D4541, and the test mechanism is shown in Figure 2. Meanwhile, the corrosion test was conducted using Palmsens4® potentiodynamic polarization based on three-electrode electrochemical cells (ASTM G3-14 standard), and the schematic diagram for this test is shown in Figure 3.

The corrosion test measurements were performed in a 3.5 wt.% NaCl solution at room temperature with Ag/AgCl as the reference electrode and Pt as the counter electrode. The Scanning rate was set at 1 mV/s, and the potential scan range was from +1.2 V to -1.2 V. Meanwhile, the equivalent weight of the tested A36 steel is 27.92 g/mol, and the density is 7.95 gr/cm<sup>3</sup>.

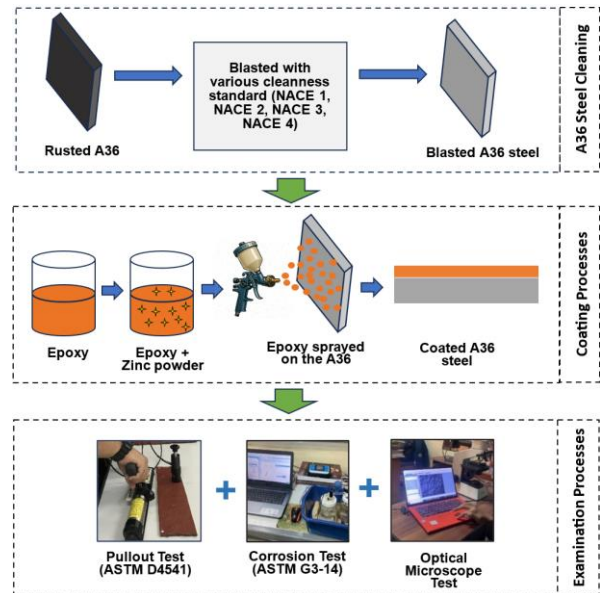


Figure 1. The research flow diagram

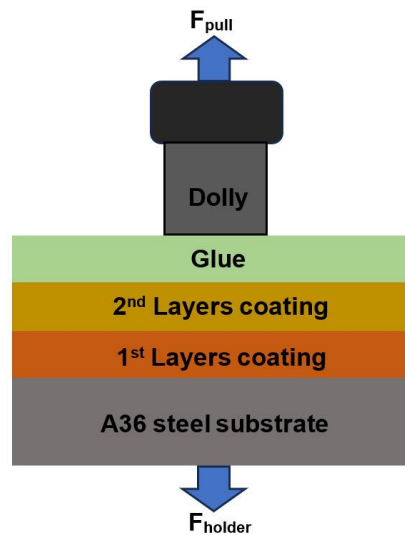


Figure 2. Pullout test Mechanism (ASTM D4541)

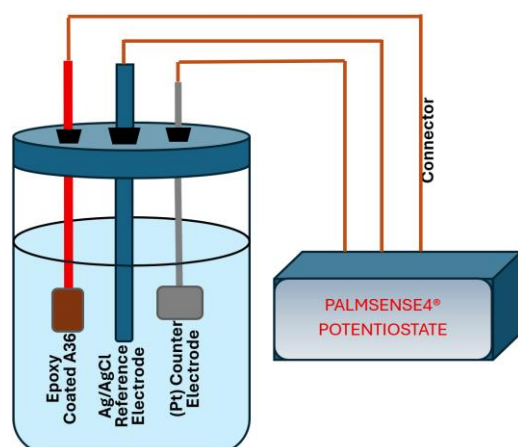


Figure 3. Potentiodynamic Test (ASTM G3-14)

## RESULTS AND DISCUSSION

### Coating cleanliness

The blasting results are illustrated in [Figure 4](#), derived from executing the blasting procedure until the target standard is attained by comparing the results with the established NACE criteria. This study employs four NACE standards: NACE 1, NACE 2, NACE 3, and NACE 4, which correspond to the specimens utilized.

The visual comparison indicates that the degree of surface cleanliness varies with the intensity and duration of the blasting treatment. The results indicate that blasting can achieve near-complete removal of rust and contaminants, especially at NACE 1 and NACE 2 levels. These higher cleanliness standards ensure an optimal surface profile for coating adhesion and corrosion resistance.



Figure 4. Blasting result of the specimen compared with the NACE standard

However, for lower cleaning standards (NACE 4 and NACE3), some residual rust and oxides remain, potentially affecting the performance of protective coatings. Blasting's ability to meet NACE 1 and NACE 2 standards suggests its suitability for high-performance coating applications.

### Coating thickness

The Coating thickness of the epoxy is shown in [Tables 1](#) and [2](#). The epoxy coating thickness data for A36 steel reveal a well-controlled and consistent application process across the different surface preparations. The data show that both layers of the epoxy coating, applied with a wet thickness of 200-250  $\mu\text{m}$ , achieve relatively consistent dry thicknesses across all specimens. In particular, the dry thickness of Layer 1 ranges from 140  $\mu\text{m}$  to 148  $\mu\text{m}$ , while that of Layer 2 ranges from 157  $\mu\text{m}$  to 163  $\mu\text{m}$ .

These slight variations are expected and reflect the normal variability in the curing process of epoxy coatings. Despite the differences in dry thickness between the layers and across surface preparations, the final average thickness values are very consistent. The final thickness ranges from 300  $\mu\text{m}$  to 305  $\mu\text{m}$ , with a mean thickness of 303.25  $\mu\text{m}$  and a minimal standard deviation of 2.04  $\mu\text{m}$ . This indicates that the epoxy coating process is highly uniform, with only minor differences between the specimens, likely due to slight variations in surface roughness resulting from different surface preparations. Surface preparation does influence the dry thickness to some extent. For example, NACE 4 has the highest dry thickness for Layer 1 (148  $\mu\text{m}$ ), while NACE 1 has the highest for Layer 2 (163  $\mu\text{m}$ ). However, these differences do not significantly affect the overall coating thickness. The minimal variation in the final average thickness across specimens suggests that, regardless of the surface preparation method used, the epoxy coating achieves a similar overall thickness.

Table 1. 1<sup>st</sup> Layer

No. Spc	Surface Prep.	1 <sup>st</sup> Layer		
		Wet thickness ( $\mu\text{m}$ )	Dry thickness ( $\mu\text{m}$ )	STD
1	NACE 4	200.0-250.0	148.0	0.816
3	NACE 3	200.0-250.0	140.0	1.633
4	NACE 2	200.0-250.0	143.0	1.414
5	NACE 1	200.0-250.0	140.0	1.632
1	NACE 4	200.0-250.0	148.0	0.816

Table 2. 2<sup>nd</sup> Layer

No. Spc	Surface Prep.	1 <sup>st</sup> Layer		
		Wet thickness ( $\mu\text{m}$ )	Dry thickness ( $\mu\text{m}$ )	STD
1	NACE 4	200.0-250.0	157.0	0.942
3	NACE 3	200.0-250.0	160.0	1.414
4	NACE 2	200.0-250.0	162.0	1.632
5	NACE 1	200.0-250.0	163.0	1.632
1	NACE 4	200.0-250.0	157.0	0.942

### Pullout Strength

The image of pullout test results is shown in [Figure 5](#), and the pullout strength data is shown in [Table 3](#). The pullout test strength data for the epoxy coating on A36 steel show varying adhesion performance depending on surface preparation technique. NACE 2 shows the highest pullout strength at 9.76 MPa, indicating superior adhesion, with 95% of failures occurring in the 2<sup>nd</sup> Layer, suggesting a strong bond between the 1<sup>st</sup> Layer and the substrate. In contrast, NACE 4 had the lowest pullout strength of 6.79 MPa, with failure predominantly in the 1<sup>st</sup> Layer, suggesting weaker adhesion between the 1<sup>st</sup> Layer and the metal substrate.

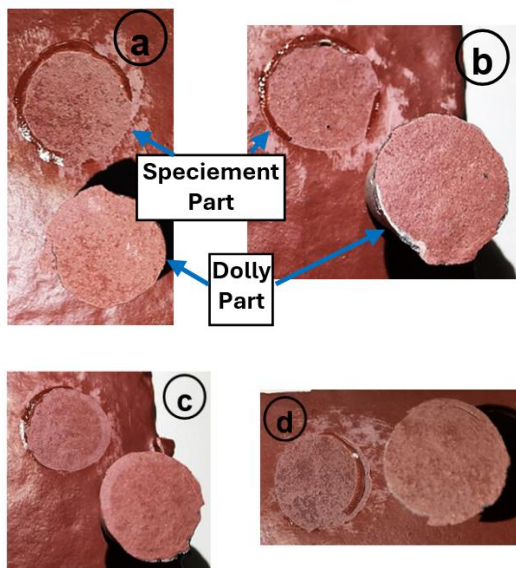


Figure 5. Post pullout of sample surface: a) NACE 4, b) NACE 3, c) NACE 2, d) NACE 1.

Table 3. Pullout Strength results

SPC No	Surface Preparation	Pullout Strength (Mpa)	STD	CV	Note (Pulled Part)
1	NACE 4	6.79	0.141	2.08%	1st = 70% 2nd = 30%
2	NACE 3	7.89	0.107	1.36%	1st = 45% 2nd = 55%
3	NACE 2	9.76	0.104	1.07%	2nd = 95% Y/Z = 5%
4	NACE 1	7.07	0.095	1.34%	1st = 35% 2nd = 65%

NACE 1 and NACE 3 exhibit moderate bond strength, with pullout strengths ranging between 7.07 MPa and 7.89 MPa, and a similar pattern of failure predominantly in the second Layer (55-65%), indicating that the bond between the first Layer and the substrate was stronger in these cases. The data underscores the importance of adequate surface preparation, with roughening techniques like those used in NACE 2 leading to enhanced adhesion and improved performance of the epoxy coating through stronger interlocking mechanisms. At the same time, other methods resulted in weaker layer bonding and lower overall strength. It should be noted that, even though the roughness is high, such as NACE 3 and NACE 4, it is also important to pay attention to the cleanliness of the blasted surface. Even with high roughness, if there are still impurities such as rust on the surface, they will reduce the pullout strength by forming a weakness point at the impurity site. The illustration of this phenomenon is shown in [Figure 6](#).

The statistical data show that NACE 2 yields the highest pullout strength (9.76 MPa), outperforming NACE 4 by +43.7%, with a low Coefficient of Variation (CV) ( $\approx 1.07\%$ ): an indication that moderate-to-high cleanliness with a preserved anchor profile optimizes the balance of cleanliness and interlocking. The failure mode's shift to the second Layer (95%) for NACE 2 further indicates that the coating–metal interface is affecting the coating performance.

### Corrosion test

The potentiodynamic polarization results for the test are shown in [Figure 7](#). This graph shows the relationship between current density and potential differences during the corrosion process.

The data reveal which specimen corrodes first. The level of ease of corrosion of a material is called the degree of nobility. Noble materials tend to be more difficult to corrode. In potentiodynamic polarization testing, this is indicated by the corrosion potential value.

Materials with a more positive corrosion potential tend to be noble, meaning they are more difficult to corrode.

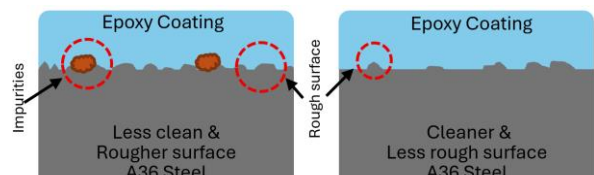


Figure 6. Illustration of coated surface A36 steel

From the data, materials with a high level of cleaning tend to be less prone to corrosion, and vice versa. Cleanliness also affects the corrosion rate, as shown in [Figure 8](#), where the most significant corrosion rate occurs in materials with a low level of cleanliness, namely NACE4. At the same time, the lowest corrosion rate occurs at the highest level of cleanliness, namely NACE 1. The corrosion rate results in NACE 1 is 0.006 mm/yr.

Meanwhile, the corrosion rate in NACE 4 is 0.056 yr. When sorted from fastest to slowest, the corrosion rates are NACE 4, NACE 3, NACE

2, and NACE 1. This is in line with the previous theory that if the surface preparation improves, the corrosion rate will be better (slower) [\[30\]](#).

This phenomenon is possible because in cleaner materials, inclusions can be minimized. Inclusions in epoxy make it more susceptible to chloride-containing electrolytes, which can trigger corrosion. This phenomenon is illustrated in [Figure 9](#). In areas where epoxy contains inclusions, the epoxy thickness may be reduced, thereby reducing its insulation against the electrolyte and allowing the electrolyte to reach the A36 steel substrate easily.

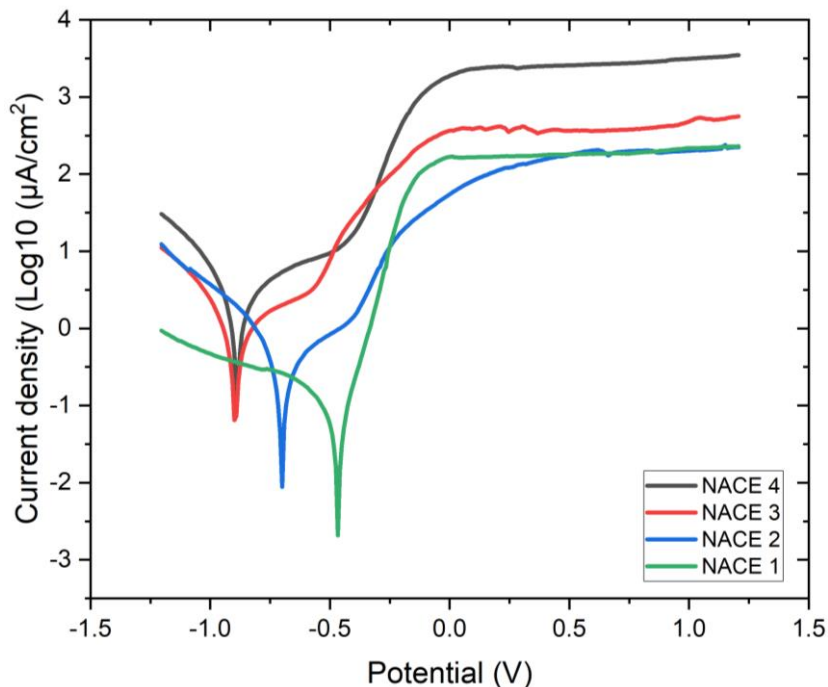


Figure 7. Potentiodynamic polarization data of coated A36 Steel

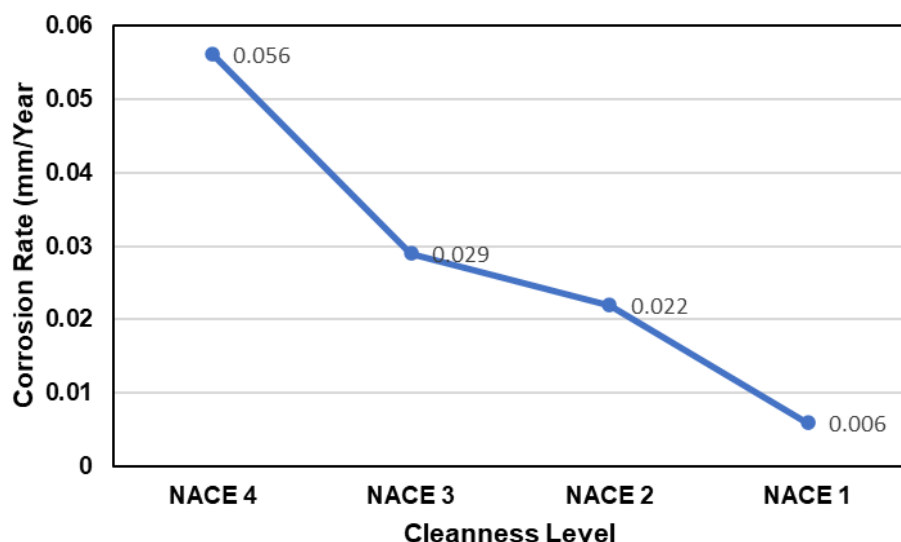


Figure 8. Corrosion rate of epoxy-coated A36 Steel

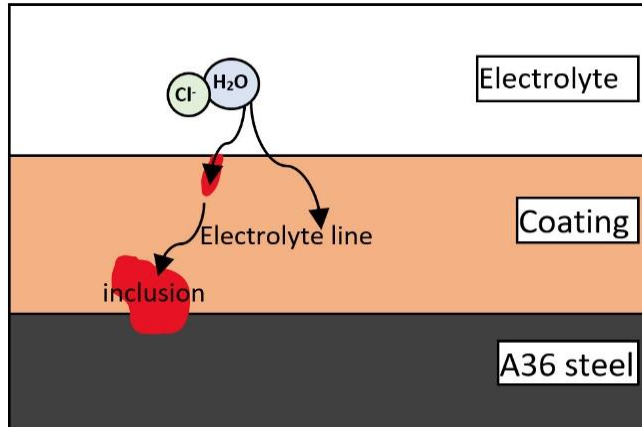


Figure 9. Electrolyte penetration in the epoxy coating scheme

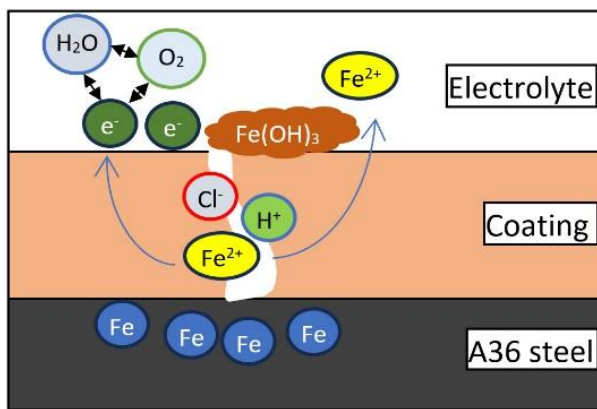
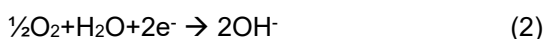


Figure 10. Corrosion processes after epoxy breakdown

This inclusion could also serve as a path for the electrolyte, as the area around it is the weakest point through which it can enter. Figure 10 illustrates the corrosion process that occurred in A36 steel after the epoxy breakdown process. In A36 steel, the main composition that occurs in corrosion is Fe, and the corrosion itself involves two primary half-reactions: oxidation and reduction. The oxidation half-reaction, referred to as the anodic reaction, involves the breakdown of the ferrous phase as follows:



According to the following, the electrons generated by the anodic reaction are consumed by the reduction half-reaction, also known as the cathodic reaction:

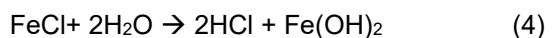


The total reaction can be written:

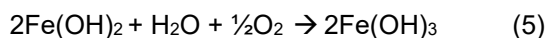


Meanwhile, the chloride ions engage with iron, and subsequently hydrolyze into

hydrochloric acid, intensifying the corrosion process and producing  $\text{Fe}(\text{OH})_2$



In the presence of oxygen and water,  $\text{Fe}(\text{OH})_2$  undergoes oxidation to transform into  $\text{Fe}(\text{OH})_3$ , as illustrated in the following reaction.  $\text{Fe}(\text{OH})_3$ , commonly known as hydrous ferric oxide, is the substance that forms rust, exhibiting a colour range from orange to reddish-brown.



The epoxy coating can be broken down by chlorine through a process called osmotic blistering. This creates an electrochemical cell with a pit (anode) on the inside and a cathode on the outside. As corrosion spreads, the area inside the hole becomes acidic and positively charged, while the surrounding area is negatively charged. This causes Chloride ions to move into the pit, lowering the pH of the solution inside it. This speeds up the corrosion rate in the pit and leads to pitting corrosion [31].

The corrosion rate trend decreases monotonically from NACE 4 to NACE 1;

compared to NACE 4 (0.056 mm/year), NACE 1 decreased to 0.006 mm/year (-89.3%). There is a powerful negative relationship between surface cleanliness and corrosion rate (Spearman  $\rho = -1$ ,  $p = 0.0417$  one-tailed;  $p = 0.0833$  two-tailed, exact test), where  $\rho$  is a monotonic relationship (-1 represents a perfect negative monotonic relationship, indicating that when the rank of one variable increases, the rank of the other variable continuously and perfectly decreases. The ranks of the variables change in the exact opposite order (from lowest to highest). This pattern is consistent with a monotonic decline from NACE 4 to NACE 1. Meanwhile, the final layer thickness was uniform ( $303.25 \pm 2.04 \mu\text{m}$ ;  $CV \approx 0.67\%$ ), thus not impacting the primary outcome.

## CONCLUSION

The surfaces prepared to the NACE 4 standard exhibited the highest dry layer thickness in the first Layer, while NACE 1 showed the greatest thickness in the second Layer. However, the overall variation in layer thickness between the specimens was minimal, indicating a consistent application process. In terms of adhesion strength, the pullout test results showed that the NACE 2 standard provided the highest pullout strength, followed by NACE 3 and NACE 1, while NACE 4 showed the lowest. This suggests that more rigorous surface preparation, as seen with NACE 2, led to stronger bonding between the coating layer and the substrate. Additionally, corrosion testing indicated that better surface preparation correlated with a lower corrosion rate. The NACE 1 standard specimen produced the best (lowest) corrosion rate, while NACE 4 exhibited the worst results. This finding confirms that improved surface preparation slows down the corrosion rate on A36 steel coated with epoxy coating. Proper surface preparation not only enhances adhesion but also provides effective corrosion protection. The best pullout strength is provided by material cleaned according to the NACE 2 standard specimen; meanwhile, for corrosion resistance, it is provided by the NACE 1 standard specimen. This research can inform ship maintenance protocols and optimize coating strategies for marine applications, especially in construction projects using A36 steel and organic coatings.

## ACKNOWLEDGMENT

We thank our colleagues from Universitas Brawijaya for their insights and expertise, which greatly assisted the research.

## REFERENCES

- [1] A. Armanfar, A. A. Tasmekepligil, R. T. Kilic, S. Demir, S. Cam, Y. Karabi, B. Abou El Majd, and E. Gunpinar, "Embedding lattice structures into ship hulls for structural optimization and additive manufacturing," *Ocean Engineering*, vol. 301, 2024, Art. no. 117601. doi: 10.1016/j.oceaneng.2024.117601.
- [2] V. M. Ngoc, N. T. Hai Ha, P. M. Ngoc, D. V. Tung, N. H. Hao, and T. N. Tu, "Numerical investigation on the influence of ship hull form modification on resistance of the 4600DWT cargo ship using RANSE method," *IOP Conference Series: Earth and Environmental Science*, vol. 1278, no. 1, Art. no. 012023, 2023. doi: 10.1088/1755-1315/1278/1/012023.
- [3] F. Pérez-Arribas, "Parametric generation of small ship hulls with CAD software," *Journal of Marine Science and Engineering*, vol. 11, no. 5, Art. no. 976, 2023. doi: 10.3390/jmse11050976.
- [4] G. Wu, S. Kong, W. Tang, R. Lei, and S. Ji, "Statistical analysis of ice loads on ship hull measured during Arctic navigations," *Ocean Engineering*, vol. 223, 2021, Art. no. 108642. doi: 10.1016/j.oceaneng.2021.108642.
- [5] D. Y. Vlasov, A. L. Bryukhanov, G. G. Nyanikova, E. A. Tsarovtseva, O. M. Yashina, and A. R. Izatulina, "The corrosive activity of microorganisms isolated from fouling of structural materials in the coastal zone of the Barents Sea," *Applied Biochemistry and Microbiology*, vol. 59, pp. 425–437, 2023. doi: 10.1134/S0003683823040166.
- [6] M. Abbas and M. Shafiee, "An overview of maintenance management strategies for corroded steel structures in extreme marine environments," *Marine Structures*, vol. 71, 2020, Art. no. 102718. doi: 10.1016/j.marstruc.2020.102718.
- [7] K. Maji and M. Lavanya, "Microbiologically influenced corrosion in stainless steel by *Pseudomonas aeruginosa*: An overview," *Journal of Bio- and Triboro-Corrosion*, vol. 10, Art. no. 16, 2024. doi: 10.1007/s40735-024-00820-w.
- [8] A. A. Al'khimenko, A. D. Davydov, A. A. Khar'kov, S. Yu. Mushnikova, O. A. Khar'kov, O. N. Parmenova, and A. A. Yakovitskii, "Methods of corrosion testing used for the development and industrial utilization of novel shipbuilding steels and alloys: A review. Part II. Corrosion cracking and marine field testing," *Steel in*

*Translation*, vol. 52, pp. 271–277, 2022. doi: 10.3103/S0967091222030020.

[9] Z. Wang, Z. Zhou, W. Xu, D. Yang, Y. Xu, L. Yang, J. Ren, Y. Li, and Y. Huang, “Research status and development trends in the field of marine environment corrosion: A new perspective,” *Environmental Science and Pollution Research*, vol. 28, pp. 54403–54428, 2021. doi: 10.1007/s11356-021-15974-0.

[10] F. Fauzri, K. Mudiono, S. Rikki, and J. Syarif, “Effect of one-year corrosion on steel bridge materials in the maintenance stage with the Charpy impact test method,” *Sinergi*, vol. 27, no. 2, pp. 153–162, 2023. doi: 10.22441/sinergi.2023.2.002.

[11] M. R. Miftakhur, A. P. Permana, and T. B. R., “Effect of forging load and heat treatment process on the corrosion behavior of A588-1%Ni for weathering steel application in a marine environment,” *Sinergi*, vol. 26, no. 2, pp. 237–248, 2022. doi: 10.22441/sinergi.2022.2.013.

[12] D. P. Dody and M. Irsyad, “Effect of ratio of surface area on the corrosion rate,” *Sinergi*, vol. 22, no. 1, pp. 7–12, 2018. doi: 10.22441/sinergi.2018.1.002.

[13] J. Li, Y. Dong, Y. Yuan, X. Zhou, Y. Liu, and X. Meng, “Recent advances of metal–organic frameworks in corrosion protection: From synthesis to applications,” *Chemical Engineering Journal*, vol. 430, 2022, Art. no. 132823. doi: 10.1016/j.cej.2021.132823.

[14] S. B. Ulaeto, R. P. Ravi, I. I. Udo, G. M. Mathew, and T. P. D. Rajan, “Polymer-based coating for steel protection, highlighting metal–organic framework as functional actives: A review,” *Corrosion Materials Degradation*, vol. 4, pp. 284–316, 2023. doi: 10.3390/cmd4020015.

[15] Y. I. Kuznetsov and G. V. Redkina, “Thin protective coatings on metals formed by organic corrosion inhibitors in neutral media,” *Coatings*, vol. 12, no. 2, Art. no. 149, 2022. doi: 10.3390/coatings12020149.

[16] I. Chopra, S. K. Ola, Priyanka, V. Dhayal, and D. S. Shekhawat, “Recent advances in epoxy coatings for corrosion protection of steel: Experimental and modelling approach—A review,” *Materials Today: Proceedings*, vol. 62, pt. 3, pp. 1658–1663, 2022. doi: 10.1016/j.matpr.2022.04.659.

[17] J. Wang, P. Du, J. Ding, J. Pu, and B. Xie, “Graphene oxide enhanced aqueous epoxy composite coating derived from sustainable cardanol resource for corrosion protection,” *Surface Topography: Metrology and Properties*, vol. 7, no. 4, pp. 1–14, 2019. doi: 10.1088/2051-672X/ab5099.

[18] W. Fürbeth, “Special issue: Advanced coatings for corrosion protection,” *Materials*, vol. 13, no. 15, Art. no. 3401, 2020. doi: 10.3390/ma13153401.

[19] S. Anwar and X. Li, “A review of high-quality epoxy resins for corrosion-resistant applications,” *Journal of Coatings Technology and Research*, vol. 21, pp. 461–480, 2024. doi: 10.1007/s11998-023-00865-5.

[20] A. Calia, S. Rossi, F. Deflorian, and M. Fedrizzi, “Recent progress in understanding filiform corrosion on organic coated steel: A comprehensive review,” *Progress in Organic Coatings*, vol. 192, 2024, Art. no. 108469. doi: 10.1016/j.porgcoat.2024.108469.

[21] S. Kim, H. Hong, T. H. Han, and M. O. Kim, “Early-age tensile bond characteristics of epoxy coatings for underwater applications,” *Coatings*, vol. 11, no. 9, Art. no. 757, 2020. doi: 10.3390/coatings9110757.

[22] S. Park, S. Kainuma, M. Yang, A. Kim, T. Ikeda, Y. Toyota, and T. Arakawa, “Advancements in abrasive water-jet treatment for efficient surface cleaning and comprehensive corrosion removal in steel structures,” *Journal of Building Engineering*, vol. 84, 2024, Art. no. 108623. doi: 10.1016/j.jobe.2024.108623.

[23] M. I. Grabarski, L. J. dos S. Lopes, G. P. da Silva, and G. Pintaude, “Evaluation of the anticorrosive painting procedure with reused abrasive for surface preparation – a case study,” *Engineering Research Express*, vol. 6, 2024, Art. no. 035018. doi: 10.1088/2631-8695/ad6af2.

[24] H. Wang, R. Yuan, X. Zhang, P. Zai, and J. Deng, “Research progress in abrasive water jet processing technology,” *Micromachines*, vol. 14, no. 8, pp. 1–33, 2023. doi: 10.3390/mi14081526.

[25] G. Sharifi, S. M. Attar, and B. Ramezanzadeh, “Effects of different surface cleaning procedures on the superficial morphology and the adhesive strength of epoxy coating on aluminium alloy 1050,” *Progress in Organic Coatings*, vol. 87, pp. 52–60, 2015. doi: 10.1016/j.porgcoat.2015.05.005.

[26] J. P. B. van Dam, S. T. Abrahami, A. Yilmaz, Y. Gonzalez-Garcia, H. Terryn, and A. Mol, “Effect of surface roughness

and chemistry on the adhesion and durability of a steel–epoxy adhesive interface,” *International Journal of Adhesion and Adhesives*, vol. 96, 2020, Art. no. 102450. doi: 10.1016/j.ijadhadh.2019.102450.

[27] A. Trentin, R. Samiee, A. H. Pakseresht, A. Durán, Y. Castro, and D. Galusek, “Influence of pre-treatments on adhesion, barrier and mechanical properties of epoxy coatings: A comparison between steel, AA7075 and AA2024,” *Applied Surface Science Advances*, vol. 18, 2023, Art. no. 100479. doi: 10.1016/j.apsadv.2023.100479.

[28] S. G. Croll, “Surface roughness profile and its effect on coating adhesion and corrosion protection: A review,” *Progress in Organic Coatings*, vol. 148, 2020, Art. no. 105847. doi: 10.1016/j.porgcoat.2020.105847.

[29] Q. Li, S. U. Nielsen, and S. Kiil, “Wettability of contaminated steel panels by water- and solvent-borne epoxy coatings: Interactions among surface tension and surface free energy components,” *Progress in Organic Coatings*, vol. 208, 2025, Art. no. 109467. doi: 10.1016/j.porgcoat.2025.109467.

[30] M. H. Shahini, H. Eivaz Mohammadloo, and B. Ramezanzadeh, “Recent advances in steel surface treatment via novel/green conversion coatings for anti-corrosion applications: A review study,” *Journal of Coatings Technology and Research*, vol. 19, pp. 159–199, 2022. doi: 10.1007/s11998-021-00466-0.

[31] B. Obereigner, G. Mayr, B. Strauß, P. Bognar, S. Ngo, K. Bretterbauer, and C. Paulik, “Key parameters and mechanism of blistering of coil-coatings in humid-hot laboratory environments,” *Progress in Organic Coatings*, vol. 175, 2023, Art. no. 107373. doi: 10.1016/j.porgcoat.2022.107373.